



# THE CATHOLIC UNIVERSITY OF AMERICA

*Department of Mechanical Engineering  
Washington, D.C. 20064  
202-635-5170*

March 9, 1990

To: Ms. Genevieve E. Wiseman  
Grant Officer  
Code 280.1  
NASA-Goddard Space Flight Center  
Greenbelt, MD 20771

---

## FINAL REPORT

---

Grant No. NAG 5-1291

Grant Title: Interaction of Minor Ions with Fast and Slow Shocks

Period Covered: October 1 to December 31, 1989

Principal Investigator: Y. C. Whang Y C Whang March 9, 1990

Department of Mechanical Engineering  
Catholic University of America  
Washington D. C., 20064

CC: NSTIF

(NASA-CR-186372) INTERACTION OF MINOR IONS  
WITH FAST AND SLOW SHOCKS Final Report, 1  
Oct. - 31 Dec. 1989 (Catholic Univ. of  
America) 34 p CSCL 03R

N90-19181

Unclas  
63/92 0269648

## Table of Contents

### Abstract

1. Introduction.....	4
2. Three-Fluid Model.....	7
2A. MHD Shocks.....	7
2B. Three Species of the MHD Fluid.....	9
2C. Lorentz Forces.....	11
2D. Jump Conditions for Alpha Particles.....	14
3. Results for Alpha Particles.....	17
3A. Computational Model.....	17
3B. Alpha Particles.....	20
4. Other Minor ions.....	22
4A. Computations.....	22
4B. Similarity Solutions for Heavy Ions.....	22
5. New Support for the Coronal Slow Shock.....	24

### Acknowledgment

### References

### Figure Captions

Abstract. The coronal slow shock has been predicted to exist embedded in large coronal holes at 4-10 solar radii. We use a three-fluid model to study the jumps in minor ion properties across the coronal slow shock. We formulate the jump conditions in the de Hoffmann-Teller frame of reference. The Rankine-Hugoniot solution determines the MHD flow and the magnetic field across the shocks. For each minor ion species, the fluid equations for the conservation of mass, momentum and energy can be solved to determine the velocity and the temperature of the ions across the shock. We also obtain a similarity solution for heavy ions. The results show that on the downstream side of the coronal slow shock the ion temperatures are nearly proportional to the ion masses for He, O, Si, and Fe in agreement with observed ion temperatures in the inner solar wind. This indicates that the possibly existing coronal slow shock can be responsible for the observed heating of minor ions in the solar wind.

## 1. Introduction.

Alpha particles and other minor ions have been extensively observed since the first measurement of the solar wind. The dynamical behavior of alpha particles and other minor ions in the solar wind is not yet well understood. The helium to hydrogen abundance ratio  $\epsilon = n_\alpha/n_p$  is highly variable. The long term average value of  $\epsilon$  is in the range of 0.03 to 0.06. The average value of the speed ratio,  $U_\alpha$  to  $U_p$ , is slightly greater than 1.00. The speed ratio,  $U_\alpha$  to  $U_p$ , near 0.3 AU is greater than that near 1 AU. The most probable value of  $T_\alpha/T_p$  is between 3 and 4. There is a strong tendency in the solar wind for the ion temperatures to be roughly proportional to the masses [Bochsler, 1989; Bochsler, et al., 1985; Hernandez, et al., 1987; Marsch, et al., 1982; Neugebauer, 1981; Neugebauer and Snyder, 1966; Ogilvie, et. al., 1968; Ogilvie, et al., 1989].

In this paper we study the jumps in flow properties for alpha particles and other minor ions across slow shocks. A few slow shocks have been identified in the solar wind [Richter, 1987], but the changes in properties of minor ions across them have not been published. Observations of changes of alpha particles velocity, density, and temperature have been published, both for fast interplanetary shocks and for the earth's bow shock [Borodkova et al., 1989; Fuselier et al., 1988; Neugebauer, 1970; Ogilvie et al., 1982; Zastenker et al., 1986]. Both Ogilvie et al. [1982] and Borodkova et al. [1989] reported that reacting to the presence of the cross-shock potential difference the alpha particles are decelerated less than the protons and a temperature-mass proportionality is introduced by the action of a fast shock. It has also been observed that magnetic forces contribute appreciably to the slowing of ions in the de Hoffmann-Teller frame of reference [Thomsen et al., 1987]. We expected that slow shocks and fast shocks may have similar effects on the dynamical

behavior of solar wind ions. This study concludes that the possibly existing coronal slow shock can be responsible for the heating of minor ions and perhaps the variation in flow velocities for different kinds of ions in the solar wind.

The coronal slow shock has been predicted to exist embedded in large coronal holes at 4-10 solar radii [Whang, 1982]. The model considers the heliomagnetic polar regions of the sun as the sources of solar wind streams, interplanetary magnetic fields of one polarity emanating from north polar cap and fields of opposite polarity from south polar cap are separated by a neutral sheet. In coronal space, the high-speed solar wind streams emanating from the polar coronal holes are sub-Alfvenic flows of low- $\beta$  plasma. Studies for the expansion of the solar wind from coronal holes in rapidly diverging stream tubes indicate that supersonic speeds should be attained at points low in the corona [Kopp and Holzer, 1976; Munro and Jackson, 1977; Whang, 1983; Whang and Chien, 1978]. Streams originating from the edge of the polar open-field regions flow around the curved boundary of the helmet-shaped, closed-field region. At the edge of the neutral sheet, the flow direction of each stream changes suddenly, becoming parallel to the neutral sheet. Due to dynamical interaction in north-south direction between neighboring stream tubes, an oblique MHD slow shock can develop near the neutral point. The shock is upstream inclined, and extends polewards to form a standing coronal slow shock surrounding the sun.

We use a three-fluid model to study the jumps in the flow properties of minor ions across slow shocks. We formulate the jump conditions in the de Hoffmann-Teller frame of reference. The Rankine-Hugoniot solution determines the MHD flow and the magnetic field across the shocks. The main body of the

paper presents a three fluid model to calculate the flow of protons and alpha particles across slow shocks under the assumption (a)  $n_\alpha$  is a small fraction of, but not negligible in comparison with,  $n_p$  and (b) the flow properties of electrons across slow shocks is specified by a polytropic relation. The model is also used to calculate the flow of other minor ions ( $^{16}\text{O}^{6+}$ ,  $^{28}\text{Si}^{8+}$  and  $^{56}\text{Fe}^{16+}$ ) across slow shocks under the limits of  $n_i \ll n_p$ .

The fluid equations for the conservation of mass, momentum and energy for each kind of ion can be solved to determine the velocity and the temperature of the ions across the shock. If the protons and each kind of minor ions ( $k = \text{He, O, Si, and Fe}$ ) have the same temperatures and the same velocities on the upstream side of a slow shock, then the model shows that under reasonable coronal conditions, on the downstream side of the coronal slow shock the calculated ion temperatures are nearly proportional to the ion masses and the average ion velocities are slightly greater than 1. Assuming that these conditions are preserved during the expansion of the solar wind between the corona and 0.3 AU, the consistent results between this study and the observations of minor ions in the inner solar wind suggest that these observations support the theoretical prediction for the existence of the coronal slow shock. We also obtain a similarity solution showing that on the downstream side of a standing slow shock the temperatures are directly proportional to masses for heavy ions.

## 2. Three-Fluid Model

### 2A. MHD Shocks

The classical Rankine-Hugoniot Relation is used to study shocks in a MHD fluid consisting of electrons, protons and alpha particles. We choose a cartesian coordinates system: the xy-plane is the plane of coplanarity, the x axis is normal to the shock surface pointing the direction of the mass flow, and the tangential component of the magnetic field points in the positive direction of the y-axis. We formulate the flow conditions in the de Hoffmann-Teller frame of reference. Outside the shock layer, the MHD fluid velocity is align with the magnetic field  $B$ , and the electric field  $E$  and the non-coplanarity component of the magnetic field  $B_z$  are zeros. Inside the shock layer  $E = Ee_x$ , and  $B$ ,  $E$ , and the fluid properties for each kind of particles ( $k = e, p$  and  $\alpha$ ) are functions of  $x$  only. This formulation includes a noncoplanarity component of the magnetic field inside the shock layer [Goodrich and Scudder, 1984; Gosling, et al., 1988; Jones and Ellison, 1987; Thomsen, et al., 1987]. The equations for the conservation of mass, momentum and energy are used to study the change in flow velocity and temperature for minor ions across the shock.

The jumps in the magnetic field  $B$  and the fluid properties  $\rho$ ,  $U$ , and  $T$  outside the shock layer can be determined by the flow conditions upstream of the shock using the Rankine-Hugoniot relation:

$$[\rho U_x] = 0 \quad (1)$$

$$\rho U_x [U] + [P + B^2/8\pi]e_x - B_x[B]/4\pi = 0 \quad (2)$$

$$[U^2/2 + c_p T] = 0 \quad (3)$$

and

$$[B_x] = 0 \quad (4)$$

Here the pair of square brackets denote the jump of a physical quantity across the shock

$$[Q] = Q_2 - Q_1 \quad (5)$$

the subscripts 1 and 2 respectively denote the flow conditions upstream and downstream of the shock.

Whang [1987] has a simple direct method to calculate the solution of the Rankine-Hugoniot relation to determine the jumps in the MHD flow and the magnetic field across oblique MHD shocks. We use this method to calculate the ratios  $B_2/B_1$ ,  $\rho_2/\rho_1$ ,  $U_{x2}/U_{x1}$ ,  $P_2/P_1$  and the shock angle  $\theta_2$ . (The shock angle  $\theta$  is the angle between the shock normal and the magnetic field). They are functions of three dimensionless upstream parameters: the shock Alfvén number  $A = U_{x1}/(a_1 \cos \theta_1)$ , the shock angle  $\theta_1$ , and the plasma  $\beta$  value. (Here  $a$  is the Alfvén speed, and  $\beta$  the ratio of the thermal pressure  $P_1$  to the magnetic pressure  $B_1^2/8\pi$ .) A shock is a slow shock if the shock Alfvén number  $A$  less than 1 and is a fast shock if  $A$  is greater than 1. The magnetic field and the shock angle decrease across a slow shock, they increase across a fast shock.

Shock solutions have been systematically studied in a three dimensional parametric space [Edmiston and Kennel, 1986; Whang, 1988]. For given  $\beta$  and  $\theta_1$ , shock solutions exist in the domain of  $A > A_{\min}$ . Here the minimum shock Alfvén number

$$A_{\min}^2 = (1 + 5\beta/6 - \{(1 + 5\beta/6)^2 - 10\beta \cos^2 \theta_1/3\}^{1/2})/2 \cos^2 \theta_1 \quad (6)$$

for slow shocks, and

$$A_{\min}^2 = (1 + 5\beta/6 + \{(1 + 5\beta/6)^2 - 10\beta \cos^2 \theta_1/3\}^{1/2})/2 \cos^2 \theta_1 \quad (7)$$



for fast shocks. Evolutionary shocks do not exist in the domain of  $A < A_{\min}$ . There are no jumps in MHD flow properties and magnetic field when  $A = A_{\min}$ . At any given value of  $\beta$ , a whole range of changes in  $B_2/B_1$ , from 0 to 1, may take place in the solution domain. The range of change in thermodynamic properties strongly depends on the  $\beta$  value. Slow shocks covering a wide range of jumps in thermodynamic properties (such as  $p$  and  $\rho$ ) exist in the low  $\beta$  region ( $\beta \leq 0.1$ ). On the other hand, only slow shocks with weak jumps in thermodynamic properties exist in the high  $\beta$  region ( $\beta \geq 1$ ). Therefore, in the coronal space where the  $\beta$  value of the solar wind is of the order of 0.1, all physical properties may jump across a slow shock over a wide range of magnitudes. Near 1 AU the plasma  $\beta$  value is in the order of 1, the jumps in thermodynamic properties across a slow shock must be small but the change in the magnetic field is not necessarily small.

In place of the shock Alfven number, shock Mach number is sometimes used as an independent variable to calculate the shock relationships. The shock Mach number is defined as the ration of  $U_n$  to the magnetoacoustic speed,  $C_s$  for slow shocks and  $C_f$  for fast shocks. In the  $M, \beta, \theta$  parameter space, slow shock solutions exist in the domain of

$$1 \leq M^2 \leq (1.2 + \beta + ((1.2 + \beta)^2 - 4.8\beta \cos^2\theta)^{1/2})/2\beta \quad (8)$$

## 2B. Three Species of the MHD Fluid

We denote the three species of the MHD fluid, electrons, protons and alpha particles, respectively by subscripts  $e$ ,  $p$  and  $\alpha$ . We consider that the number density of alpha particles  $n_\alpha$  is a small fraction of, but not negligible in comparison with the proton number density  $n_p$ . Inside the shock layer the charge density is in the order of  $(h/\delta)^2 n_e e$ , where  $h$  is the Debye shielding

distance and  $\delta$  measures the shock thickness. Since  $h \ll \delta$ , we may assume that to the zeroth order of magnitude

$$n_e = n_p + 2n_\alpha \quad (9)$$

In the de Hoffmann-Teller frame of reference, the electric field inside the shock layer is generated entirely by the charge separation which is a first order quantity. Now we can express the density and the flow velocity of the fluid consisting of three kinds of charged particles as

$$\rho = m_p n_p (1 + 4\epsilon) \quad (10)$$

$$U = \frac{U_p + 4\epsilon U_\alpha}{1 + 4\epsilon} \quad (11)$$

Since this study is concerned with different velocities and temperatures for alpha particle and protons, we should introduce the diffusion velocities

$$W_\alpha = U_\alpha - U \quad (12)$$

and

$$W_p = U_p - U$$

They are respectively the velocities of alpha particles and protons in a frame of reference moving at the fluid velocity  $U$ .  $W_p$  is expected to be very small compared with  $W_\alpha$ . Depending on the frame of references, there are two pressure tensors for alpha particles:  $(P_\alpha^*)_{ii}$  the  $ii$  component of the pressure tensor in the frame of reference moving at the fluid velocity  $U$ , and  $(P_\alpha)_{ii}$  in the frame of reference moving at the flow velocity of alpha particle  $U_\alpha$ ,

$$(P_\alpha^*)_{ii} = (P_\alpha)_{ii} + m_\alpha n_\alpha W_{\alpha i}^2 \quad (13)$$

A similar relationship exists between  $(P_p^*)_{ii}$  and  $(P_p)_{ii}$ . The fluid pressure

calculated from the Rankine-Hugoniot equations is the average of pressure tensor in the fluid frame of reference

$$P = \frac{1}{3} \sum_i \{ (P_\alpha^*)_{ii} + (P_p^*)_{ii} + (P_e^*)_{ii} \} \quad (14)$$

On the other hand, the temperatures of alpha particles and protons are respectively defined in the frame of reference moving at flow velocities of alpha particles and protons. Namely

$$n_\alpha k T_\alpha = \frac{1}{3} \sum_i (P_\alpha)_{ii} \quad (15)$$

and

$$n_p k T_p = \frac{1}{3} \sum_i (P_p)_{ii}$$

From these relations, we obtain that the fluid pressure

$$P = k(n_p T_p + n_\alpha T_\alpha + n_e T_e) + \frac{1}{3} (m_p n_p W_p^2 + m_\alpha n_\alpha W_\alpha^2) \quad (16)$$

In the next two subsections, we will develop a three-fluid model to calculate the flow of alpha particles across slow shocks. The equations for the conservation of mass, momentum and energy are used to calculate the change in  $n_\alpha$ ,  $U_\alpha$  and  $T_\alpha$ . Once we have the solutions for the alpha particles and for the MHD fluid, then we can calculate  $n_p$ ,  $T_p$ , and  $U_p$ .

## 2C. Lorentz Forces

Inside the shock layer, the electromagnetic field exerts a Lorentz force on each kind of charge particles ( $k = e, p, \alpha$ )

$$L_k = Z_k n_k e E + \frac{1}{c} J_k \times B \quad (17)$$

where  $Z_e = -1$ ,  $Z_p = 1$ ,  $Z_\alpha = 2$ , and  $e$  is the elementary charge. This force and its work done on the moving plasma affect the momentum flux and the energy

flux of the charged particles across the shock layer. Note that the parallel component of the electric current density makes no contribution to the Lorentz forces. We may express the Lorentz force as the sum of two parts

$$L_k = L_k^E + L_k^M \quad (18)$$

The first part  $L_k^E$  represents the electric Lorentz force due to the electric field and the electric drift current density and second part  $L_k^M$  is the magnetic Lorentz force due to perpendicular electric current caused by the sudden change in the magnetic field configuration inside the shock layer.

We can express the Lorentz force due to the electric field and the electric drift current density as

$$L_k^E = Z_k n_k e \{ E + (E \times B) \times B/B^2 \}$$

or

$$L_k^E = Z_k n_k e E \cos \theta e_1 \quad (19)$$

where  $e_1 = B/B$  is the unit vector along the field direction. Summing over all kinds of charged particles,

$$\sum_k L_k^E = 0 \quad (20)$$

This means that the electric Lorentz force produces no net effect on jumps of fluid properties for the MHD fluid, the mixture of all kinds of charged particles, as shown in the Rankine-Hugoniot equations.

Making use of Ampere's law, the sum over all kinds of charged particles of the Lorentz forces caused by the magnetic field configuration inside the shock layer must be equal to  $(\nabla \times B) \times B/4\pi$

$$\sum_k L_k^M = (\nabla \times B) \times B/4\pi \quad (21)$$

Integration of this equation over the shock layer produces the accumulated effects of the Lorentz forces which appears in the Rankine-Hugoniot equation (2). Equation (21) provides an important constraint the magnetic Lorentz force  $L_k^M$ . However, it is difficult to formulate the exact expression for each  $L_k^M$ . Our scheme is using the guiding-center theory to estimate the ratios  $L_e^M : L_p^M : L_\alpha^M$ , then can obtain a reasonably representation for each of them from (21).

The perpendicular electric current densities driven by the magnetic field configuration can be calculated from the motion of the guiding centers which are the instantaneous centers of the particle orbits. (The parallel component of the electric current density makes no contribution to the Lorentz forces.) Using the gyration theory of charged particles we can describes the effect of the changing magnetic field configuration on the motion of the guiding center. For each kind of charged particle there are three electric current densities related to the magnetic field configuration: the gradient drift current, the curvature drift current and the magnetization current. From these drift current densities, we can obtain the portion of  $J_{\perp k}$  driven by the magnetic field configuration as

$$J_{\perp k} = \frac{c}{B} (P_{\parallel k} - P_{\perp k}) \mathbf{e}_1 \times \boldsymbol{\kappa} \quad (22)$$

where  $\boldsymbol{\kappa} = \mathbf{e}_1 \cdot \nabla \mathbf{e}_1$  is the curvature vector,  $\parallel$  and  $\perp$  refer to directions relative to the local magnetic field.  $\boldsymbol{\kappa}$  points the instantaneous center of the circular arc and the radius of curvature equals to  $1/\kappa$ . This equation shows that the perpendicular electric current density  $J_{\perp k}$  ( $k = p, \alpha, e$ ) inside the shock layer is directly proportional to the thermal pressure anisotropy  $(P_{\parallel k} - P_{\perp k})$ . Since the electrons are nearly thermally isotropic, our model assumes that

$$L_e^M = 0 \quad (23)$$

Based on this formulation, we can obtain an estimate for the following ratios

$$L_p^M : L_\alpha^M = (P_{\parallel p} - P_{\perp p}) : (P_{\parallel \alpha} - P_{\perp \alpha}) \quad (24)$$

From Equations (21), (23) and (24) we obtain

$$L_k^M = \Gamma_k (\nabla \times B) \times B / 4\pi \quad (25)$$

for  $k = p$  and  $\alpha$  where

$$\Gamma_p = \frac{P_{\parallel p} - P_{\perp p}}{(P_{\parallel p} - P_{\perp p}) + (P_{\parallel \alpha} - P_{\perp \alpha})} \quad (26)$$

$$\Gamma_\alpha = \frac{P_{\parallel \alpha} - P_{\perp \alpha}}{(P_{\parallel p} - P_{\perp p}) + (P_{\parallel \alpha} - P_{\perp \alpha})} \quad (27)$$

## 2D. Jump Conditions for Alpha Particles

The equations for conservation of mass, momentum and energy for alpha particles can be integrated to give

$$[n_\alpha U_{\alpha x}] = 0 \quad (28)$$

$$[n_\alpha m_\alpha U_{\alpha x}^2 + n_\alpha k T_\alpha] = F_\alpha \quad (29)$$

$$[n_\alpha m_\alpha U_{\alpha x} U_{\alpha y}] = G_\alpha \quad (30)$$

and

$$[U_\alpha^2/2 + 5kT_\alpha/2m_\alpha] = -Z_\alpha e[\phi]/m_\alpha \quad (31)$$

where

$$F_{\alpha} = \int \left( Z_{\alpha} n_{\alpha} e E \frac{B_x^2}{B^2} - \Gamma_{\alpha} \frac{d}{dx} \left( \frac{B^2}{8\pi} \right) \right) dx \quad (32)$$

$$G_{\alpha} = \int \left( Z_{\alpha} n_{\alpha} e E \frac{B_x B_y}{B^2} + \Gamma_{\alpha} \frac{B_x}{4\pi} \frac{dB_y}{dx} \right) dx \quad (33)$$

and  $\phi$  is the electrostatic potential. The term on the right hand side of Equation (31) represents an energy sink. The alpha particles do work as they move against the electrostatic field inside the shock layer.  $F_{\alpha}$  and  $G_{\alpha}$  are respectively the integration of  $L_{\alpha x}$  and  $L_{\alpha y}$  across the shock layer. They represent the accumulated effects of the Lorentz forces over the shock layer on the momentum flux of alpha particles. The first parts of  $F_{\alpha}$  and  $G_{\alpha}$  shows that alpha particles are decelerated by the electric Lorentz forces. The second parts of  $F_{\alpha}$  and  $G_{\alpha}$  represents the effects of the magnetic Lorentz forces on alpha particles. Inside a slow shock, the magnetic Lorentz forces accelerate alpha particles in the shock normal direction and decelerate alpha particles in the tangential direction. Slow shocks occur in low  $\beta$  plasma such as in the solar coronal or in the geomagnetic tail environment. Equations (32) and (33) show that except for parallel shocks the magnetic Lorentz forces normally play an more important role than the electric Lorentz forces in affecting the dynamical behavior of alpha particles crossing slow shocks. The integrations for the z component of the momentum equations are not shown here because they only produce first order corrections to the flow speeds.

Equations (28)-(31) are used to calculate the ratios  $n_{\alpha x 2}/n_{\alpha x 1}$ ,  $U_{\alpha x 2}/U_{\alpha x 1}$ ,  $U_{\alpha y 2}/U_{\alpha y 1}$  and  $T_{\alpha 2}/T_{\alpha 1}$  across the shock layer. We can first use (31) to calculate the jump in tangential velocity across the shock

$$[U_{\alpha y}] = \frac{G_{\alpha}}{m_{\alpha} n_{\alpha 1} U_{\alpha x 1}} \quad (34)$$

Then we solve Equations (28), (29) and (31) for  $n_{\alpha x2}/n_{\alpha x1}$ ,  $U_{\alpha x2}/U_{\alpha x1}$  and  $T_{\alpha 2}/T_{\alpha 1}$ . The system of equations can be reduced to a quadratic equation for  $U_{\alpha x2}/U_{\alpha x1}$

$$(U_{\alpha x2}/U_{\alpha x1})^2 - \lambda_1(U_{\alpha x2}/U_{\alpha x1}) + \lambda_0 = 0 \quad (35)$$

where

$$\lambda_1 = \frac{5}{4} \left( 1 + \frac{kT_{\alpha 1}}{m_{\alpha} U_{\alpha x1}^2} + \frac{F_{\alpha}}{m_{\alpha} n_{\alpha 1} U_{\alpha x1}^2} \right) \quad (36)$$

$$\lambda_0 = \frac{1}{4} - \frac{[U_{\alpha y}^2]}{4U_{\alpha x1}^2} + \frac{5kT_{\alpha 1}}{4m_{\alpha} U_{\alpha x1}^2} - \frac{Z_{\alpha} e[\phi]}{2m_{\alpha} U_{\alpha x1}^2} \quad (37)$$

The equation has two roots associated with the  $\pm$  signs of the square root term. The solution with  $-$  sign represents the shock solution. This step produces the most important dynamical effect of shock wave on alpha particles: part of the kinetic energy is converted to increase the thermal energy. Once we have  $U_{\alpha x2}/U_{\alpha x1}$ , we can calculate  $n_{\alpha 2}/n_{\alpha 1}$ ,  $T_{\alpha 2}/T_{\alpha 1}$  from

$$n_{\alpha 2}/n_{\alpha 1} = U_{\alpha x1}/U_{\alpha x2} \quad (38)$$

and

$$T_{\alpha 2} = T_{\alpha 1} - (m_{\alpha}/5k)[U_{\alpha}^2] - (2Z_{\alpha} e/5k)[\phi] \quad (39)$$



### 3. Results for Alpha Particles

#### 3A. Computational Model

Section 2 provides a theoretical formulation for the jumps in flow properties of protons and alpha particles across slow shocks. The same formulation can be used to calculate the jump of other minor ions across slow shocks (in section 4) and to calculate the jump of ions across fast shocks (in a separate paper). In order to carry out numerical computations, we need to make three further assumptions with regard to (a) the flow conditions upstream of the shock, (b) the electron flow across the shock, and (c) the thermal anisotropy of protons and alpha particles. Note that once we have better understanding about electron flow and thermal anisotropy of ions, the theoretical formulation obtained in this paper can be upgraded to carry out new calculations.

We assume that on the upstream side of the shock all kinds of particles have the same flow velocity and the same fluid temperature

$$T_{\alpha 1} = T_{p1} = T_{e1} \quad (40)$$

and

$$U_{\alpha 1} = U_{p1} = U_{e1} \quad (41)$$

We assume that inside the shock layer the thermodynamic properties of electrons may be described by a polytropic relation

$$P_e = P_{e1}(n_e/n_{e1})^\gamma \quad (42)$$

or

$$T_e = T_{e1}(n_e/n_{e1})^{\gamma-1}$$

where  $\gamma$  is the polytropic index ranging between 5/3 and 3 [Feldman, 1985;

Schwartz, et al., 1987; Schwartz, 1988; Scudder, 1987; Thomsen, et al., 1987]. Computations carried out in this paper use  $\gamma = 5/3$ . Although the electrons carry a significant parallel electric current, the parallel electric current makes no contribution to the Lorentz forces. According to the gyration theory of charged particles, the Lorentz force induced by the magnetic field configuration on electrons is negligible because the electrons are nearly isotropic [Equation (23)]. In the equation of motion for electrons, the inertia term is negligible because the electron kinetic energy is much less than the electron thermal energy. The x-component of the equation of motion for electrons can be reduced to

$$\frac{dP_e}{dx} = - n_e e E \cos^2 \theta \quad (43)$$

Under the polytropic law one can calculate the electrostatic potential rise across a shock from (43)

$$e[\phi] = \gamma k \langle \cos^2 \theta \rangle [T_e] / (\gamma - 1). \quad (44)$$

Here the pair of angle brackets denote the average value of a physical quantity inside the shock layer.

We assume that the distribution functions of the solar wind alpha particles and protons have similar asymmetries with respect to the magnetic field line. The alpha particle thermal anisotropy is generally slightly, but perhaps not significantly lower than that for protons near 1 AU [Bosqued et al., 1977; Hundhausen et al., 1970; Marsch et al. 1982; Ogilvie et al., 1980]. The ratios  $P_{\parallel p}/P_{\perp p}$  and  $P_{\parallel \alpha}/P_{\perp \alpha}$  can be functions of x. If we assume that  $P_{\parallel p}/P_{\perp p} = P_{\parallel \alpha}/P_{\perp \alpha}$ , then we can write (26) and (27) as

$$\Gamma_p = \frac{P_p}{P_p + P_\alpha} \quad (45)$$

$$\Gamma_\alpha = \frac{P_\alpha}{P_p + P_\alpha} \quad (46)$$

Now, we can express the integrals for  $F_\alpha$  and  $G_\alpha$  in the following form:

$$F_\alpha = -Z_\alpha \left\langle \frac{n_\alpha}{n_e} \right\rangle [P_e] - \langle \Gamma_\alpha \rangle \frac{[B_y]^2}{8\pi} \quad (47)$$

and

$$G_\alpha = -Z_\alpha \left\langle \frac{n_\alpha B_y}{n_e B_x} \right\rangle [P_e] + \langle \Gamma_\alpha \rangle \frac{B_x [B_y]}{4\pi} \quad (48)$$

Since we do not know the detailed structure of the flow and field inside the shock layer, we have to use an approximate method to estimate those average values of physical properties which appear in equations (44), (47) and (48). We use the average of the values on the two sides of the shock layer to represent the average, namely  $\langle Q \rangle = (Q_1 + Q_2)/2$ . If  $Q_2$  is an unknown variable of the equation system, an iteration scheme is used to calculate the average values.

We calculate the flow conditions downstream of slow shocks, with a particular interest in the two ratios  $T_{\alpha 2}/T_{p 2}$ , and  $U_{\alpha 2}/U_{p 2}$ . For a given combination of the plasma  $\beta$  value, the shock angle  $\theta_1$ , and a dimensionless shock speed, the shock Mach number or the shock Alfvén number  $A = U_{x1}/(a_1 \cos \theta_1)$ , we first calculate the ratios  $B_2/B_1$ ,  $\rho_2/\rho_1$ ,  $U_{x2}/U_{x1}$ ,  $U_{y2}/U_{y1}$ ,  $T_2/T_1$  and  $\theta_2$  using the simple direct method of Whang [1987] for the MHD Rankine-Hugoniot relation. Then we calculate the flow conditions of alpha particles for the ratios  $n_{\alpha 2}/n_{\alpha 1}$ ,  $U_{\alpha x 2}/U_{\alpha x 1}$ ,  $U_{\alpha y 2}/U_{\alpha y 1}$  and  $T_{\alpha 2}/T_{\alpha 1}$  across the shock layer

following the method developed in section 2D for a given the initial helium to hydrogen abundance ratio  $\epsilon_1 = n_{\alpha 1}/n_{p1}$ . The third step is to calculate the flow conditions of protons using formulas developed in section 2C. The solutions can be organized as functions of four dimensionless parameters:  $\beta$ ,  $\theta_1$ ,  $\epsilon_1$  plus A or M.

### 3B. Alpha Particles

The shock relations formulated in the de Hoffmann-Teller frame of reference have a singularity at  $\theta_1 = 90^\circ$ . The iteration scheme also becomes difficult to converge for nearly perpendicular shocks. We carry out numerical solutions for  $0^\circ \leq \theta_1 \leq 60^\circ$ . For a given combination of  $\beta$  and  $\epsilon_1$ , we can construct constant contour plots for  $T_{\alpha 2}/T_{p2}$  and  $U_{\alpha 2}/U_{p2}$  on  $M, \theta_1$  plane as shown in Figures 1 and 2. The thick lines represent the constant contours for  $T_{\alpha 2}/T_{p2}$  and thin lines for  $U_{\alpha 2}/U_{p2}$ . The two panels in Figure 1 show that the variation in the helium to hydrogen abundance ratio,  $\epsilon_1 = 0.05$  and  $0.10$ , produces very insignificant changes for  $T_{\alpha 2}/T_{p2}$  and  $U_{\alpha 2}/U_{p2}$ . The domain of solution for slow shocks is bounded on the right by a curve representing  $M = M_{\max}$ . Slow shocks are evolutionary for  $1 \leq M \leq M_{\max}$ . Four contour plots with varying  $\beta$  values are shown in Figure 2. The plasma  $\beta$  value has a stronger effect on the solutions of  $T_{\alpha 2}/T_{p2}$  and  $U_{\alpha 2}/U_{p2}$ . The variation in  $\beta$  substantially changes the upper limit of the slow Mach number. As  $\beta$  changes from  $0.01$  to  $0.20$ ,  $M_{\max}$  decreases from  $\approx 11.0$  to  $\approx 2.5$ . At very small  $\beta$ ,  $M_{\max}$  varies as  $\sqrt{(1.2/\beta)}$ .

The flow parameters upstream of the coronal slow shock may be estimated to be in the range of  $\beta \approx 0.02$ ,  $M > 3.0$  and  $15^\circ \leq \theta_1 \leq 45^\circ$  [Whang, 1982, Figure 1]. From Figure 2, we find that immediately downstream of the coronal slow shock the temperature ratio  $T_\alpha/T_p$  should be in the range between 3 to 4 and the average speed ratio  $U_\alpha/U_p$  should be slightly greater than 1. The ion

temperatures approximately proportional to the ion masses can be expected to preserve between the corona and 0.3 AU.

#### 4. Other Minor Ions

##### 4A. Computations

The three-fluid model can be used to calculate the conditions of other minor ions across a slow shock. In this case the MHD fluid consists of electrons  $e$ , protons  $p$  and a species of minor ions  $i = {}^{16}\text{O}^{6+}$ ,  ${}^{28}\text{Si}^{8+}$ ,  ${}^{56}\text{Fe}^{16+}$  or others. We can assume that  $n_i \ll n_p$ . Under this assumption, we can use  $n_p = n_e$ ,  $U_p = U$ , and  $\Gamma_i = \langle P_i/P_p \rangle$  in the computation. Figures 3-5 shows the contour plots for the ratios  $U_{i2}$  to the fluid velocity  $U_2$  and  $T_{i2}$  to fluid temperature  $T_2$  respectively for  ${}^{16}\text{O}^{6+}$ ,  ${}^{28}\text{Si}^{8+}$  and  ${}^{56}\text{Fe}^{16+}$  at two  $\beta$  values. Once again these figures show that the temperature ratio proportional to ion mass is the most important dynamical effect of shock wave on minor ions. The coronal slow shock convert a part of the kinetic energy to increase the thermal energy. A careful examination of Figures 4 and 5 reveals a striking result that the constant contours for  $U_{i2}$  and  $T_{i2}/m_i$  are almost identical in these plots.

##### 4B. Similarity Solutions for Heavy Ions

For heavy minor ions, because  $Z_i$  is much greater than 1 Equations (32) and (34) show that the magnetic Lorentz force becomes less important as compared with the electric Lorentz force. Because  $m_i$  is much greater than  $m_p$ , in the upstream side of the slow shock the thermal energy is much less than the kinetic energy. If we neglect these small order terms, then we can arrange the jump conditions for heavy ions in the following form:

$$\frac{n_{i2}}{n_{i1}} U_{ix2} = U_{x1} \quad (49)$$

$$\frac{n_{i2}}{n_{i1}} \left( U_{ix2}^2 + \frac{kT_{i2}}{m_i} \right) = U_{x1}^2 + \frac{Z_i}{m_i} \int \frac{n_i}{n_{i1}} eE \frac{B_x^2}{B^2} dx \quad (50)$$

$$\frac{n_{i2}}{n_{i1}} U_{ix2} U_{iy2} - U_{x1} U_{y1} + \frac{Z_i}{m_i} \int \frac{n_i}{n_{i1}} e E \frac{B_x B_y}{B^2} dx \quad (51)$$

and

$$\frac{U_{i2}^2}{2} + \frac{5}{2} \frac{kT_{i2}}{m_i} = \frac{U_1^2}{2} - \frac{Z_i}{m_i} e[\phi] \quad (52)$$

Here we have a system of four equations for four unknowns  $n_{i2}/n_{i1}$ ,  $U_{ix2}$ ,  $U_{iy2}$ , and  $kT_{i2}/m_i$ . In the limit of  $n_i \ll n_p$ , protons and electrons are responsible for the setting up of the electric field inside the shock layer and the variation of the magnetic field across the shock layer. If we consider two kinds of heavy ions having the same ratios  $Z_i/m_i$  across the same shock wave, the two flows are governed by the same system of four equations. All corresponding terms on the right hand sides of the two systems are identical. The two equation systems have the same solutions. The two flows are described by a set of similarity solutions. This similarity relationship explains that no noticeable differences exist between the computational results in Figure 4 for Si and in Figure 5 for Fe. The similarity solution for  $kT_i/m_i$  means that across the coronal slow shock the temperatures are proportional to the masses for heavy ions.

## 5. New Support for the Coronal Slow Shock

We use the fluid equations for the conservation of mass, momentum and energy to describe the ion flow across a postulated coronal slow shock predicted to occur in the low  $\beta$  coronal space between 4 and 10 solar radii. From figures 1 - 5 we can see that on the downstream side of the coronal slow shock, for He, O, Si, and Fe the ion temperatures are approximately proportional to the ion masses and the average ion velocities are slightly greater than the proton velocity. The result is consistent with the ion temperatures and velocities observed in the inner solar wind. We infer this result as a new support for the possible existence of coronal slow shocks.

If the coronal slow shock indeed exists, our understanding of the solar wind process will be significantly revised. There exists one illustrative example which calculates the solar wind flow associated with the possibly existing coronal slow shocks [Whang, 1986]. The example has calculate a strong latitudinal variation of the solar wind, the terminal speed at the pole is greater than that at the equator by a factor of 2 and the plasma density at the pole is less than that at the equator by a factor of three. The low-density and high-speed solar wind at the pole region should be directly observable from Ulysses spacecraft.

The support provided by this study of minor ions across slow shocks should stimulate modelers to consider the coronal slow shock in their solar wind models. A systematic study of coronal slow shocks should produce more quantitative solutions from which we can estimate the range of variation for important shock parameters such as the position and the shock strength and identify the range of coronal conditions under which the coronal slow shocks may exist. Because the predicted coronal slow shock is within the reach of the



future Solar Probe spacecraft, continued theoretical studies of the coronal slow shock will become very helpful in the planning of the Solar Probe mission and its experiments.

## REFERENCES

- Bochsler, P., J. Geiss, and R. Jews, Kinetic temperatures of heavy ions in the solar wind, J. Geophys. Res., 90, 10,779-10,789, 1985.
- Bochsler, P., Velocity and abundance of silicon ions in the solar wind, J. Geophys. Res., 94, 2365-2373, 1989.
- Borodkova, N. L., Y. I. Yermolaev, and G. N. Zastenker, Motion of the strong disturbances in the interplanetary medium, Cospar Colloquium on Physics of the Outer Heliosphere, Warsaw, 1989.
- Bosqued, J. M., C. D'Uston, A. A. Zertzalov, and O. L. Vaisberg, Solar Phys., 51, 231, 1977.
- Edmiston, J. P., and C. F. Kennel, A parametric study of slow shock Rankine-Hugoniot solutions and critical Mach numbers, J. Geophys. Res., 91, 1361-1372, 1986.
- Feldman, W. C., Electron velocity distributions near collisionless shocks, in Collisionless Shocks in the Heliosphere: Reviews of Current Research, Geophys. Monogr. Ser., vol.35, edited by B. T. Tsurutani and R. G. Stone, p.195, AGU, Washington, D.C., 1985.
- Fuselier, S. A., E. G. Shelley, and D. M. Klumpar, AMPTE/CCE observations of shell-like  $\text{He}^{2+}$  and  $\text{O}^{6+}$  distributions in the magnetosheath, Geophys. Res. Lett., 15, 1333-1336, 1988.
- Goodrich, C. C. and J. D. Scudder, The adiabatic energy change of plasma electrons and the frame dependence of the cross-shock potential at collisionless magnetosonic shock waves, J. Geophys. Res., 89, 6654-6662, 1984.
- Gosling, J. T., D. Winske, and M. F. Thomsen, Noncoplanar magnetic fields at collisionless shocks: A test of a new approach, J. Geophys. Res., 93, 2735-2740, 1988.
- Hernandez, R., S. Livi, and E. Marsch, On the  $\text{He}^{2+}$  to  $\text{H}^+$  temperature ratio in slow solar wind, J. Geophys. Res., 92, 7723-7727, 1987.

- Hundhausen, A. J., S. J. Bames, J. R. Asbridge, and S. J. Sydorik, J. Geophys. Res., 75, 4643, 1970.
- Kopp, R. A., and T. E. Holzer, Dynamics of coronal holes region I. steady polytropic flows with multiple critical points, Solar Phys., 49, 43, 1976.
- Jones, F. C., and D. C. Ellison, Noncoplanar magnetic fields, shock potentials, and ion deflection, J. Geophys. Res., 92, 11,205-11,207, 1987.
- Marsch, E., K.-H. Muehlhaeuser, H. Rosenbauer, R. Schwenn, F. M. Neubauer, solar wind helium ions: Observations of the Helios solar probes between 0.3 and 1 AU, J. Geophys. Res., 87, 35-52, 1982.
- Munro, R., and B. Jackson, Physical properties of a polar coronal hole from 2 to 5  $R_{\odot}$ , Astrophys. J., 213, 874, 1977.
- Neugebauer, M., Initial deceleration of solar wind positive ions in the earth's bow shock, J. Geophys. Res., 75, 717, 1970.
- Neugebauer, M., Observations of solar wind helium, Cosmic Physics, 7, 131-199, 1981.
- Neugebauer, M., and C. W. Snyder, Mariner 2 observations of the solar wind, J. Geophys. Res., 71, 4469-4479, 1966.
- Ogilvie, K. W., L. F. Burlaga, and Wilkerson, Plasma observations on Explorer 34, J. Geophys. Res., 21, 6809-6819, 1968.
- Ogilvie, K. W., P. Bochsler, M. A. Coplan, and J. Geiss, Observations of the velocity distribution of solar wind ions, J. Geophys. Res., 85, 6069-6074, 1980.
- Ogilvie, K. W., M. A. Coplan, and R. D. Zwickl, Helium, hydrogen, and oxygen velocities observed on ISEE-3, J. Geophys. Res., 87, 7363-7369, 1982.
- Ogilvie, K. W., M. A. Coplan, P. Bochsler, and J. Geiss, Solar wind observations with the Ion Composition Instrument aboard the ISEE-3(ICE) spacecraft, Sol. Phys., in press, 1989.

- Richter, A. K., Interplanetary slow shocks: a review, Proc. 6th Intern. Solar Wind Conf., NCAR/TN-306, 411, 1987.
- Schwartz, S. J., M. F. Thomsen, and W. C. Feldman, Electron dynamics and potential jump across slow mode shocks, J. Geophys. Res., 92, 3165-3174, 1987.
- Schwartz, S. J., M. F. Thomsen, S. J. Bame, and J. Stansberry, Electron heating and the potential jump across fast mode shocks, J. Geophys. Res., 93, 12923-12931, 1988.
- Scudder, J. D., The field-aligned flow approximation for electrons within layers possessing a normal mass flux: a corollary to the de Hoffmann-Teller theorem, J. Geophys. Res., 92, 13,447-13,455, 1987.
- Thomsen, M. F., J. T. Gosling, S. J. Bame, K. B. Quest, and D. Winske, On the noncoplanarity of the magnetic field within a fast collisionless shock, J. Geophys. Res., 92, 2305-2314, 1987.
- Whang, Y. C., Slow shocks around the sun, Geophys. Res. Lett., 9, 1081-1084, 1982.
- Whang, Y. C., Expansion of the solar wind from a two-hole corona, Solar Phys., 88, 343-358, 1983.
- Whang, Y. C., Solar wind flow upstream of the coronal slow shock, Astrophys. J., 307, 838-846, 1986.
- Whang, Y. C., Slow shocks and their transition to fast shocks in the inner solar wind, J. Geophys. Res., 92, 4349-4356, 1987.
- Whang, Y. C., Evolution of interplanetary slow shocks, J. Geophys. Res., 93, 251-255, 1988.
- Whang, Y. C., and T. H. Chien, Expansion of the solar wind in high-speed streams, Astrophys. J., 221, 350, 1978.
- Zastenker, G. N., O. Vaisberg, V. Smirnov, A. Skalsky, N. Borodkova, Yu Yemolavev, Solar wind protons, alphas and electrons at the bow shock and the potential barrier, 26th COSPAR abstract 6.2.8, 1986.

### Figure Captions

Fig. 1 The thick lines represent the constant contours for  $T_{\alpha 2}/T_{p 2}$  and thin lines for  $U_{\alpha 2}/U_{p 2}$ . The two panels show that the variation in  $\epsilon_1$  produces very insignificant changes for  $T_{\alpha 2}/T_{p 2}$  and  $U_{\alpha 2}/U_{p 2}$ .

Fig. 2. Four contour plots for slow shocks with  $\epsilon_1 = 0.05$  and  $\beta = 0.01, 0.02, 0.10$  and  $0.20$  show that the plasma  $\beta$  value has a strong effect on the solutions of  $T_{\alpha 2}/T_{p 2}$  and  $U_{\alpha 2}/U_{p 2}$ .

Fig. 3. The three-fluid model is used to calculate the conditions of other minor ions across a slow shock. Two contour plots show the ratios  $U_{i 2}/U_2$  and  $T_{i 2}/T_2$  for  $i = {}^{16}\text{O}^{6+}$  with  $\beta = 0.01$  and  $0.1$ .

Fig. 4. Two contour plots for  $i = {}^{28}\text{Si}^{8+}$  with  $\beta = 0.01$  and  $0.1$ . The ion temperature ratio proportional to ion mass is the most important dynamical effect of shock wave on minor ions.

Fig. 5. Two contour plots for  $i = {}^{56}\text{Fe}^{16+}$  with  $\beta = 0.01$  and  $0.1$ . We also obtain a similarity solution for heavy ions to explain the reason that no noticeable differences exist between the computational results in Figure 4 for Si and in Figure 5 for Fe.

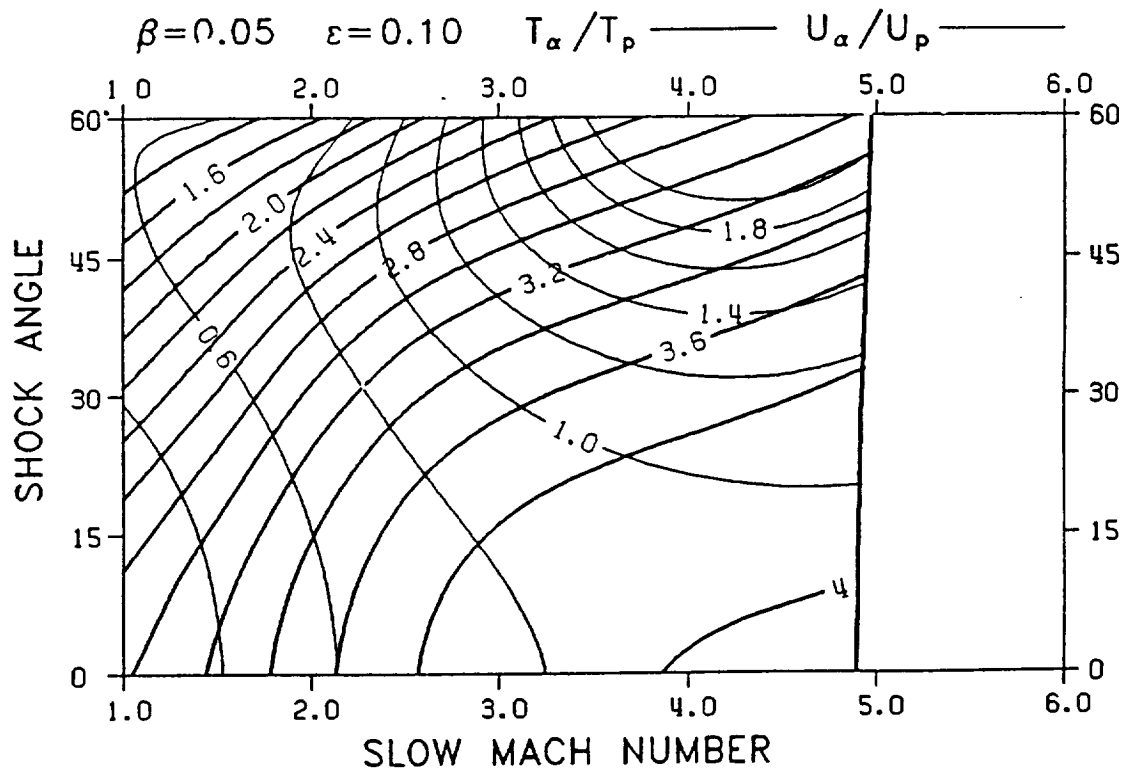
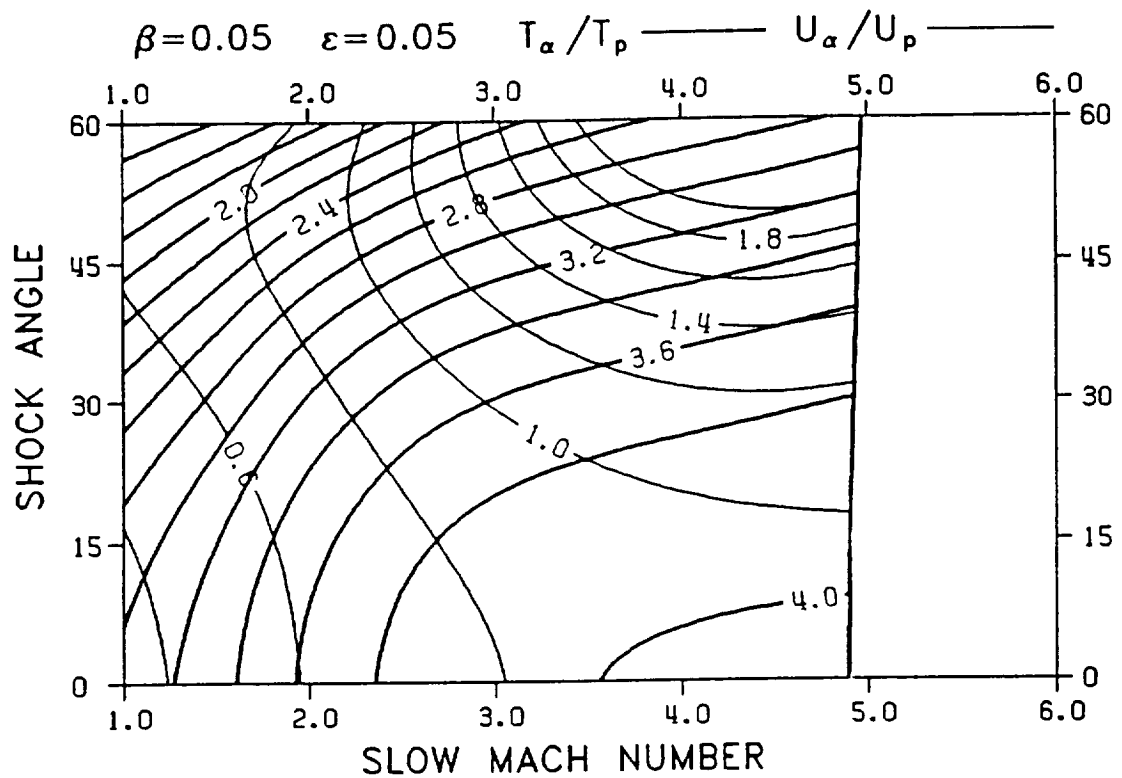


Fig. 1 The thick lines represent the constant contours for  $T_{\alpha 2}/T_{p 2}$  and thin lines for  $U_{\alpha 2}/U_{p 2}$ . The two panels show that the variation in  $\varepsilon_1$  produces very insignificant changes for  $T_{\alpha 2}/T_{p 2}$  and  $U_{\alpha 2}/U_{p 2}$ .

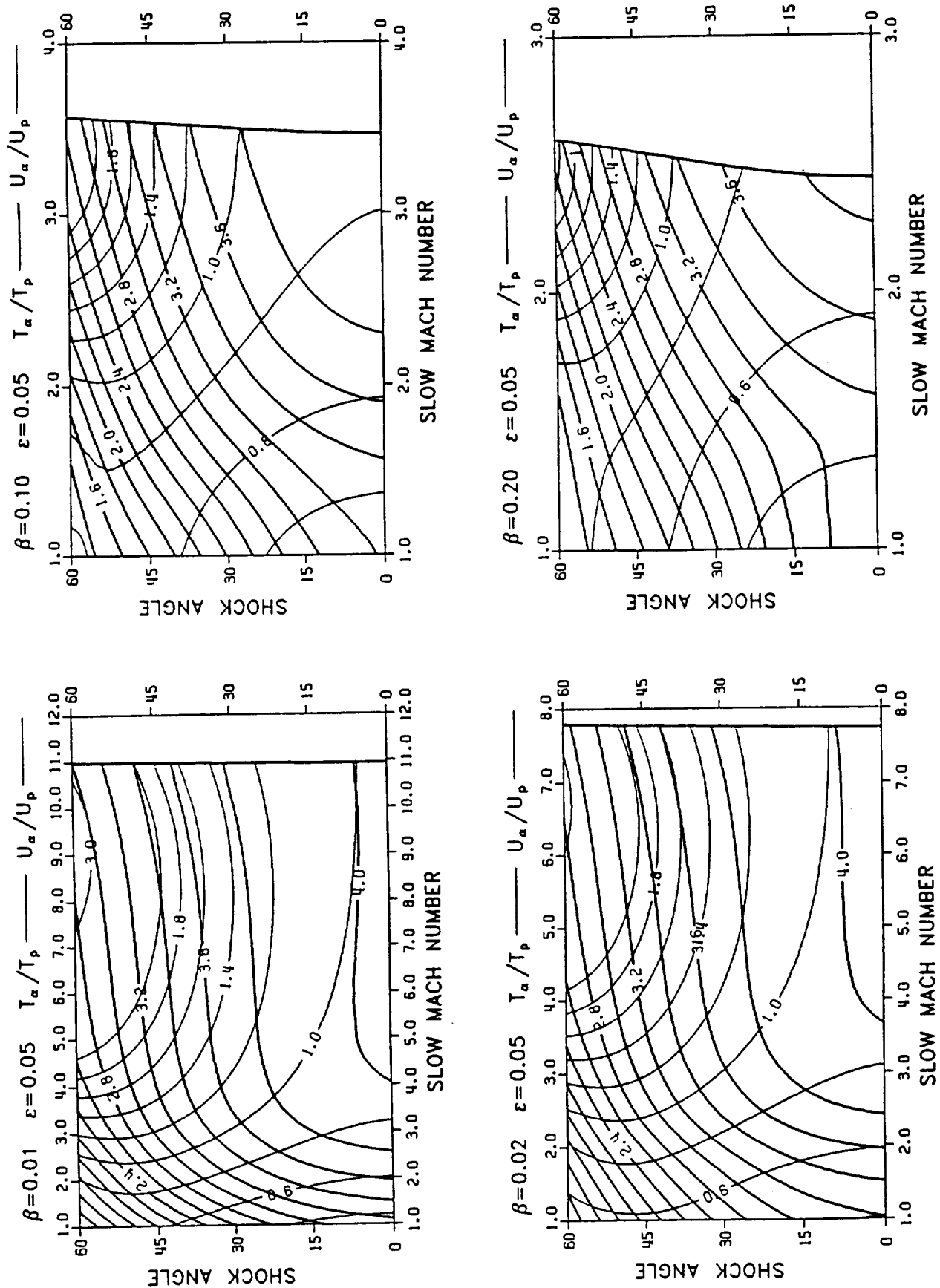


Fig. 2. Four contour plots for slow shocks with  $\epsilon_1 = 0.05$  and  $\beta = 0.01, 0.02, 0.10$  and  $0.20$  show that the plasma  $\beta$  value has a strong effect on the solutions of  $T_a/T_p$  and  $U_a/U_p$ .

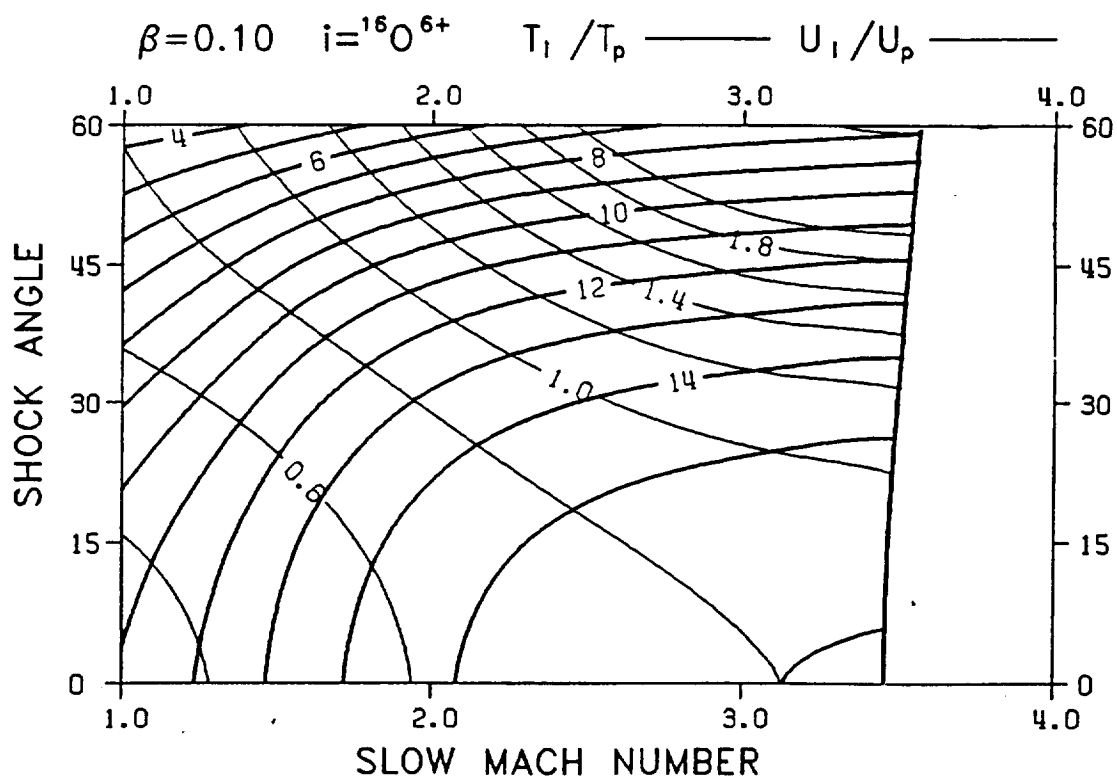
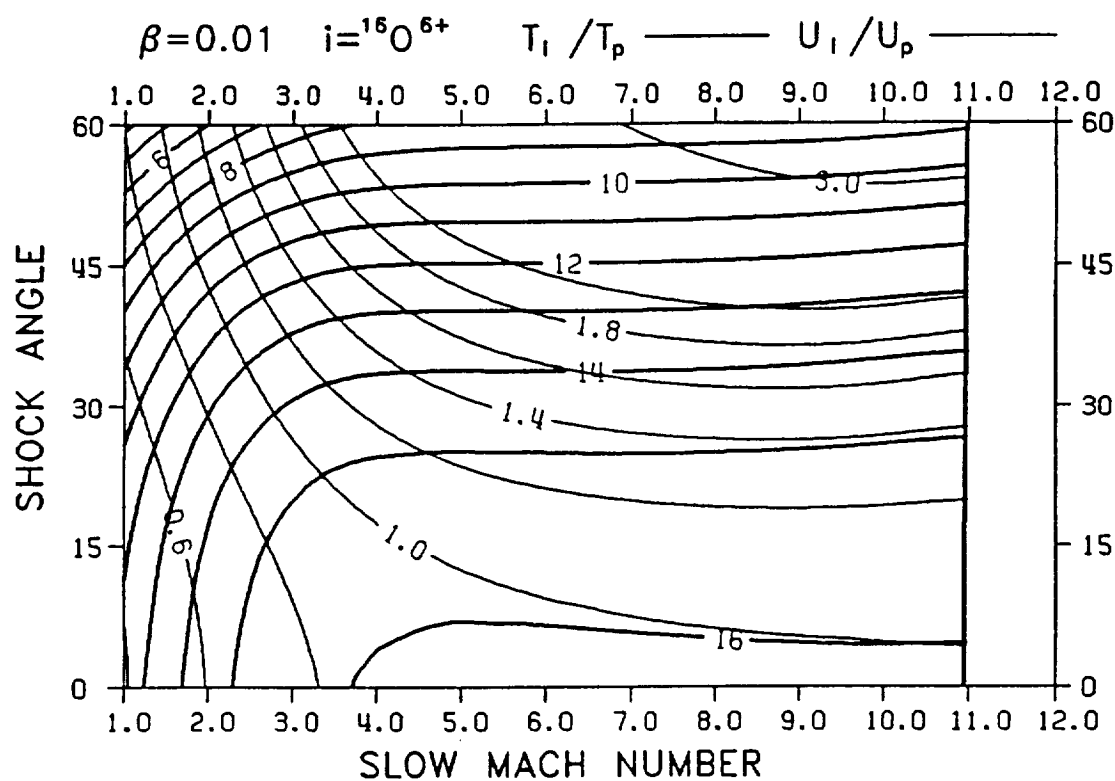


Fig. 3. The three-fluid model is used to calculate the conditions of other minor ions across a slow shock. Two contour plots show the ratios  $U_{i2}/U_2$  and  $T_{i2}/T_2$  for  $i = {}^{16}\text{O}^{6+}$  with  $\beta = 0.01$  and  $0.1$ .



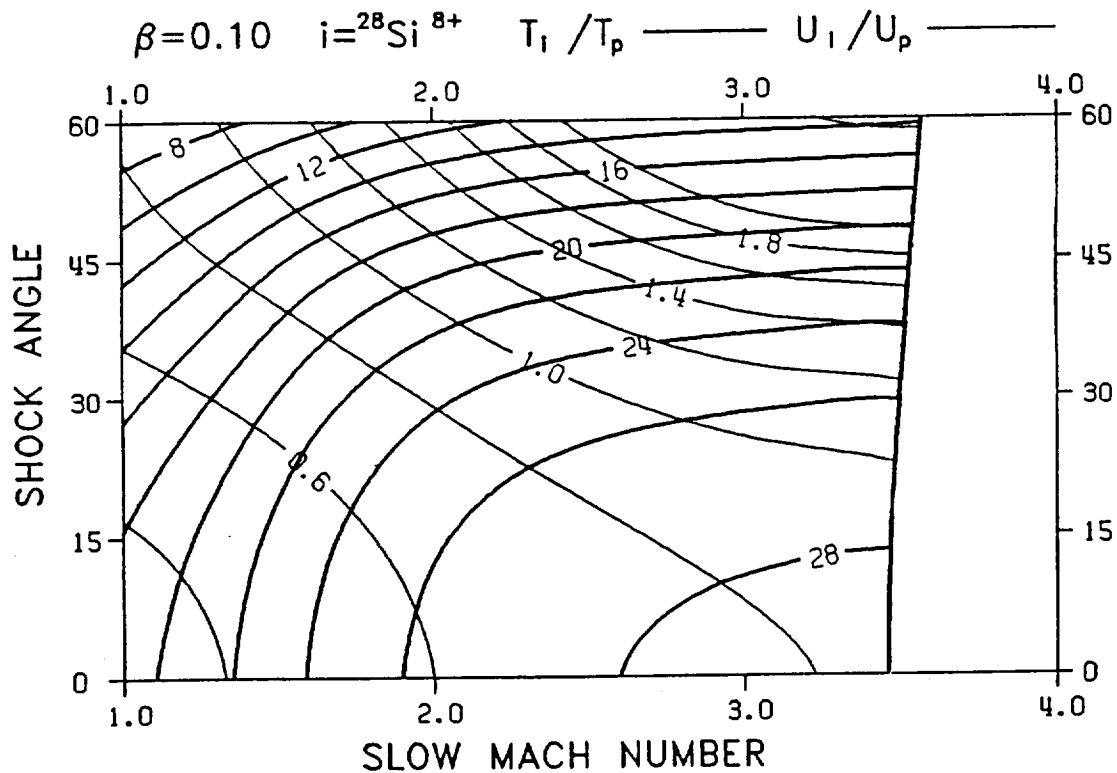
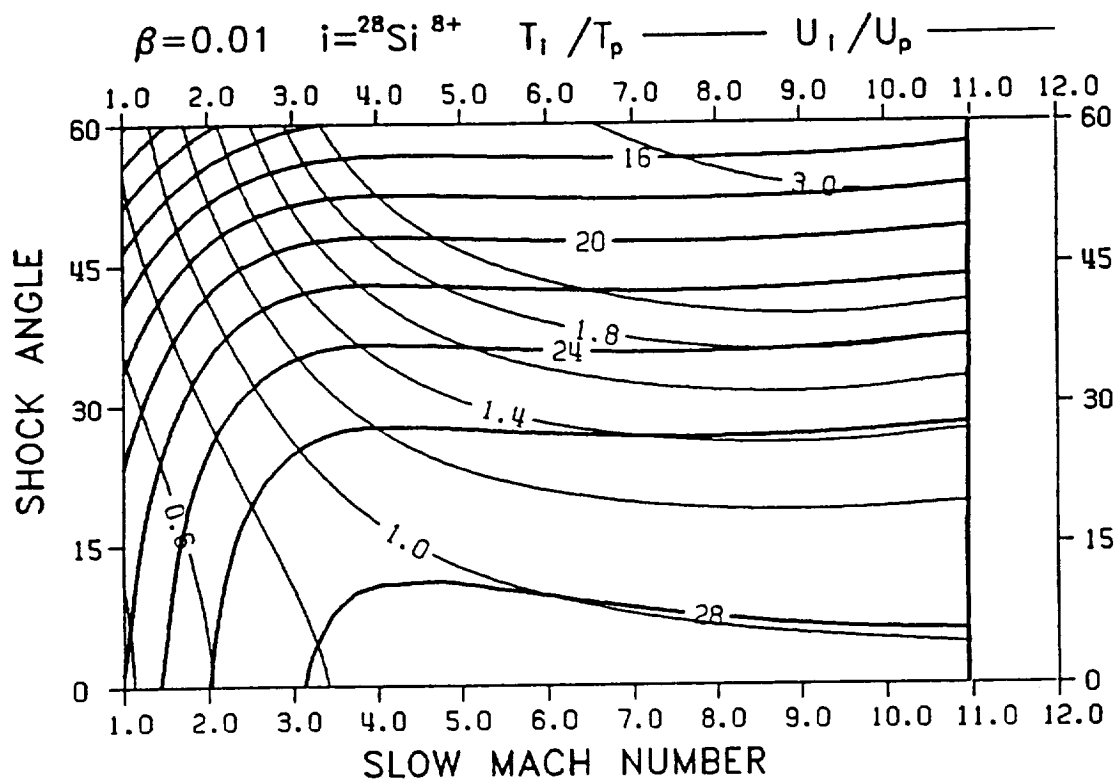


Fig. 4. Two contour plots for  $i = {}^{28}\text{Si}^{8+}$  with  $\beta = 0.01$  and  $0.1$ . The ion temperature ratio proportional to ion mass is the most important dynamical effect of shock wave on minor ions.

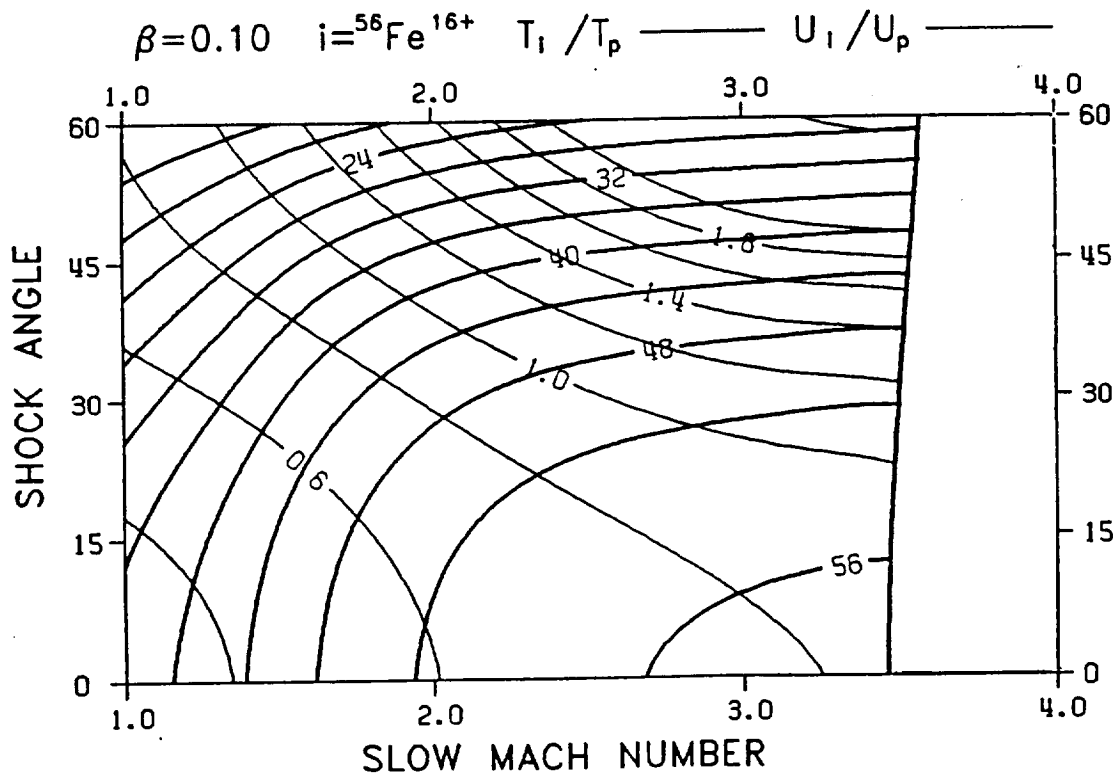
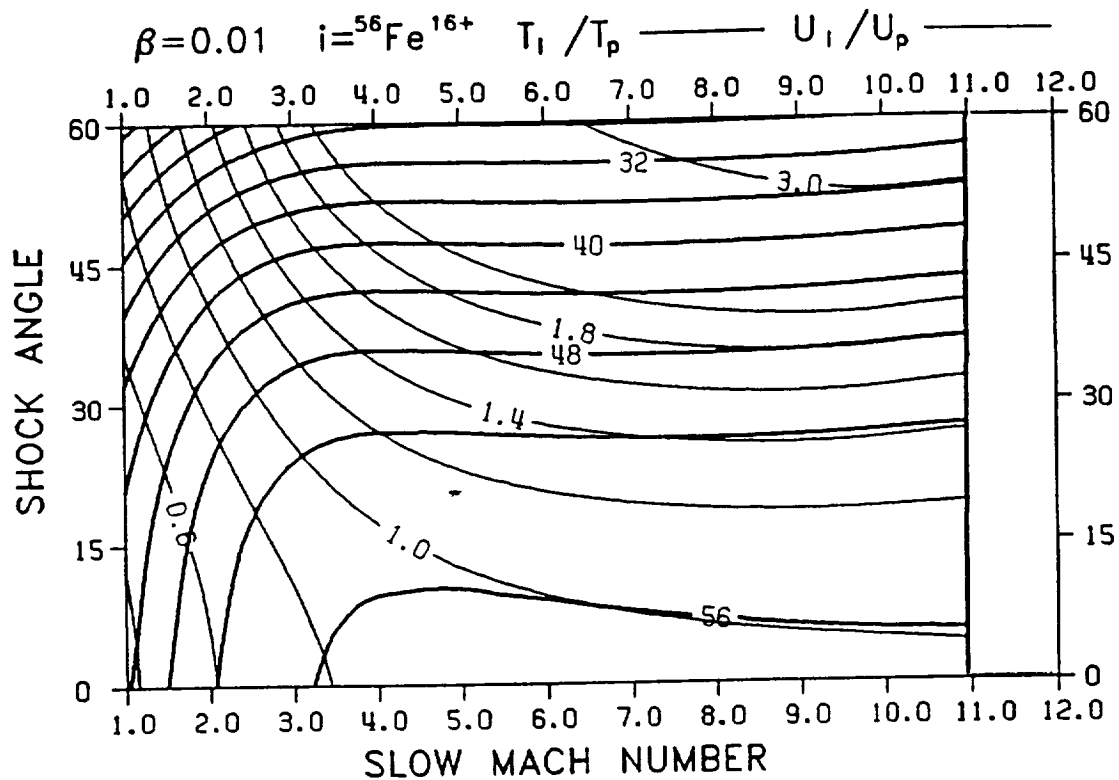


Fig. 5. Two contour plots for  $i = {}^{56}\text{Fe}^{16+}$  with  $\beta = 0.01$  and  $0.1$ . We also obtain a similarity solution for heavy ions to explain the reason that no noticeable differences exist between the computational results in Figure 4 for Si and in Figure 5 for Fe.